0038-075C/02/16701-1–8
Soil Science

January 2002
Vol. 167, No. 1
Printed in U.S.A.

TECHNICAL ARTICLES

INFILTRATION MEASUREMENT USING A VERTICAL TIME-DOMAIN REFLECTOMETRY PROBE AND A REFLECTION SIMULATION MODEL

Dennis Timlin[1] and Yakov Pachepsky[2]

Experimental methods are needed to measure infiltrations at several locations simultaneously during rainfall or irrigation. The objective of this study was to test the feasibility of using a time domain reflectometry (TDR) probe installed vertically into the soil to track the propagation of the wetting front during infiltration. We used a numerical method to simulate wave traces. The dielectric constant above the wetting front and the probe characteristics were known. The trace simulation method was coupled to a nonlinear optimization program to fit the apparent lengths of the TDR probe above and below the wetting front and the dielectric constant of the soil below the wetting front. The optimization program employed a genetic algorithm. The progression of the wetting front into the soil was recorded as a function of the apparent length of the section of the TDR probe above the wetting front. Direct measurements of the wetting front advance were obtained from observations of infiltration in a clear acrylic cylinder packed with soil and ponded with water. The root mean square errors of the predicted wetting front depths did not exceed 0.4 cm. The method shows promise in estimating wetting front depth as a function of time. (Soil Science 2002;167:1–8)

Key words: TDR probe, wetting front, infiltration, simulation.

SIMPLE techniques are needed to quantify infiltration of water into soil. Either surface influx of water or changes in the soil water distribution profile during infiltration are measured with existing techniques (Ahuja et al., 1976). Changes in the soil water distribution profile, in particular, will affect wave traces from a time domain reflectometry probe inserted into the soil vertically where infiltration occurs. The impedance mismatch between the wet soil behind the wetting front and the dry soil ahead of the front, will cause a change in the wave trace when the reflection from the wetting front reaches the TDR device. A technique developed to detect this impedance change accurately could be used to measure the wetting front advance as well as cumulative infiltration.

Time domain reflectometry instruments are highly versatile and have been used in different ways to study infiltration. Topp and Davis (1981) used TDR to measure infiltration of water through cracks in soil. Parkin et al. (1995) used measurements of average water content along a vertically installed TDR probe to calculate infiltration under constant flux conditions. They then used this information to estimate unsaturated soil hydraulic conductivity. Si et al. (1999) extended the method of Parkin et al. (1995) and utilized probes that measured both water content and soil matric potential. Probes of varying length were installed and the infiltration rate was calculated

[1]USDA-ARS Alternate Crops and Systems Laboratory, Bldg. 001, Rm 342, 10300 Baltimore Ave, Beltsville, MD 20705. Dr. Timlin is corresponding author. E-mail: dtimlin@asrr.arsusda.gov

[2]USDA-ARS Hydrology and Remote Sensing Laboratory, Beltsville, MD 20705.

Received Jan. 3, 2001; accepted Sept. 4, 2001.

from the change in average water contents along the probes.

Strong nonuniformity in water distribution along TDR waveguides is reflected in the wave trace. Several studies have investigated the use of TDR in nonuniformly wetted soils. The purpose of some of these studies was to look at errors in TDR measurements of water content when soil water content varied with depth or in layered profiles. Topp et al. (1982) reported that when water content varied with depth, the TDR gave a measure of the average water content. In a later study, Topp and Davis (1985) investigated the use of TDR probes with discontinuities to provide boundaries along the probe and allow accurate measurement of water content at different depths using probes installed vertically in soil. The discontinuities were used to determine the proportion of waveguide length in each section of soil along the rods. Hence, water content in various depths along the waveguide could be distinguished. They found, however, that peaks associated with some of the discontinuities were not always detectable, especially those close to the ends of the waveguides.

The sequence of wet over dry or dry over wet is known to affect the ability to detect a discontinuity in water content along the waveguide (Dasberg and Hopmans, 1992). Nadler et al. (1991) report that where a wet soil overlies a dry soil, the apparent length may be measured as longer than its water content indicates, using conventional wave analysis methods.

Recently, Timlin and Pachepsky (1996) developed a TDR wave trace simulation program that calculated wave traces from characteristic impedances and apparent dielectric coefficients of the TDR probe and soil. The objective of this study was to evaluate the feasibility of using a TDR wave trace simulation program to track the progress of a wetting front in soil along a TDR probe during infiltration.

MATERIALS AND METHODS

Infiltration Experiment

A 40-cm-tall, 14-cm-ID clear acrylic column was packed uniformly with a topsoil from Bourne fine sandy loam (Fine-loamy, mixed, semiactive, thermic Typic Fragiudults). A TDR probe was inserted vertically into the soil in the center of the cylinder. The value of K'_d, the apparent dielectric coefficient of the dry soil, was obtained from a trace measurement before infiltration began. A 5-cm ponded depth of water was applied and allowed to infiltrate into the soil. During infiltration, the ponded depth of water was recorded, and the wetting front progression was marked out on the wall of the clear cylinder. The wetting front was uniform around the circumference of the cylinder and did not appear to vary more than 0.5 cm between the maximum and minimum depths. Cumulative infiltration and infiltration rate were recorded from this data. The cumulative infiltration was adjusted for the volume of the TDR probe handle covered by water. Bulk densities and initial water contents are given in Table 1 along with the value of the apparent dielectric coefficients for dry soil, (K'_d).

Time Domain Reflectometer Measurements

Wave traces were recorded using a Tektronix 1502B cable tester and a 30-cm TDR probe with three parallel waveguides. The cable tester was controlled and waveforms recorded by a Campbell Scientific SDM-50 module connected to a CR-10 data logger. Wave traces were recorded every 30 s for the first 30 min and every 60 s until the end of the infiltration period (25 to 60 min). A subset of about half these measurements was used to fit the wetting front parameters to limit the amount of time to fit the parameters. These were chosen manually to represent the changing conditions of the infiltration event with a minimum of duplication.

Simulation Method

The method is described here briefly. For more information please refer to Timlin and Pachepsky (1996). To simulate a trace with the multiple reflection model, it is necessary to subdivide the transmission line into small segments and to calculate reflected and transmitted voltages at the segment boundaries for a sequence of time increments. Each homogeneous section of the transmission line, i.e., cable, handle, and waveguides (rods) is characterized by three parameters: intrinsic impedance Z, the apparent dielectric constant K', and the length of the section L. The

TABLE 1

Initial conditions for the two infiltration experiments. θ_f is total porosity (from bulk density). K'_d is the apparent dielectric constant of the soil at the initial water content.

Infiltration no.	Bulk density	θ_f	θ_i	Air filled porosity (ϕ)	K'_d
	g cm^{-3}	---------- cm^3 cm^{-3} ----------			
1	1.0	0.63	0.10	.53	3.2
2	1.2	0.55	0.06	.49	2.1

time increment to calculate reflected and transmitted voltages is equal to the time step between two voltages sampled by the TDR. Lengths of the segments along the transmission line are selected to allow the wave to pass the segment exactly twice during one time increment. Segments have the same length within a homogeneous section of the transmission line (i.e. cable, handle, or rods), and the segment length varies from one section to another because the velocity of the wave propagation differs. Reflected voltages that return to the voltage propagation source (TDR) are accumulated for each value of time, and the simulated TDR trace is the summation of these accumulated voltages as a function of time.

The rise time of the TDR, which results in dispersion of the waveform, is accounted for by including a "damping" effect (Timlin and Pachepsky, 1996). Attenuation of the signal (Δf_i) in a segment of transmission line (i) is modeled as (Yanuka et al., 1988):

$$\Delta f_i = \exp(-\alpha_i L_i) \tag{1}$$

where L_i is the length of the transmission line segment. The value of α, in theory, is dependent on the bulk electrical conductivity of the soil. Bulk electrical conductivity can be expressed as a function of water content and solid phase conductivity (Dasberg and Dalton, 1985). Since the exact water content is unknown, α is modeled in this work as a function of the apparent dielectric constant (K′), with the relationship between the apparent dielectric constant and water content (θ) from Ledieu et al. (1986):

$$\alpha = a\sqrt{K'} \tag{2}$$

The coefficient a is unknown *a priori* and has to be found from experimental wave traces along with dielectric constants of rods and handles.

The assumptions of the model are: (i) the wetting front is diffuse and moves uniformly downward; (ii) the water contents ahead of the wetting front and behind the wetting front are constant during infiltration; and (iii) signal attenuation caused by conductance is constant along the waveguide.

The wetting front is actually never sharp, and the width of the wetting front zone increases as the wetting depth increases. There are analytical solutions for finding water content as a function of depth within the wetting front zone (Kirkham and Powers, 1972). However, they require knowledge of soil hydraulic properties. To avoid the need to measure water retention and hydraulic conductivity, we use an approximate, diffusion-like spread equation to mimic the shape of the wetting front zone (Kirkham and Powers, 1972):

$$K'_x = K'_d + (K'_w - K'_d)\, erfc\left[\frac{x - D_u}{2\sqrt{\beta t}}\right] \quad x \geq D_u$$
$$K'_x = K'_w \qquad x < D_u \tag{3}$$

Where K'_x is the apparent dielectric constant of the waveguide at distance x from the handle; K'_d and K'_w are the apparent dielectric constants of the soil ahead of the wetting front and behind the wetting front, respectively; D_u is the location of the upper boundary of the wetting front where the soil water content begins to decrease from its satiated value; and β is the diffusivity parameter. The position of the upper boundary of the wetting front, D_u, is assumed to depend on time according to a power law relationship (Ali and Swartzendruber, 1994):

$$D_u = s\, t^c \tag{4}$$

Here water content is assumed to be constant and equal to the satiated value from the surface to this depth, t is time, and s and c are coefficients. The depth of the wetting front ($D_\star$) is assumed to correspond to the depth of the dielectric constant that is at the approximate midpoint between K'_w and K'_d:

$$D_\star = D_u + \sqrt{\beta t} \tag{5}$$

This gives a value of 0.5 for the term inside the complementary error function of Eq. (3) when $D_\star$ is equal to x (the value of complementary error function for 0.5 is 0.48).

Figure 1 shows an example of distributions of K′ as a function of depth generated using Eq. (3). The depth of the approximate midpoint K′ (Eq. (5)) that corresponds to the visual demarcation between wet and dry soil visible in the soil core is shown in the figure.

Fitting the Simulated Wave Trace to the Measured One

The parameters to be fitted were (a) the apparent dielectric constant K'_w of soil above the wetting front, (b) parameters of the wetting front propagation c, s, β in Eqs. (3) and (4), (c) impedances of the handle and rods, and (d) attenuation coefficient, a in Eqs. (1) and (2), above the wet-

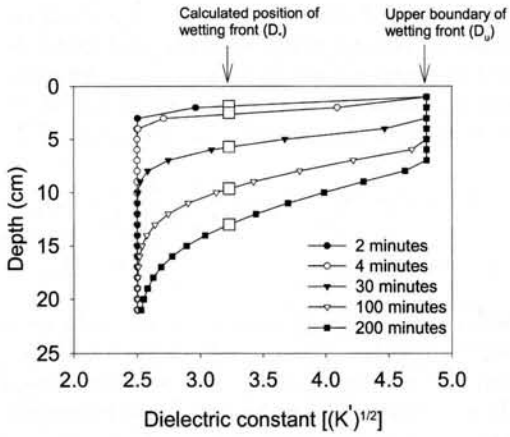

Fig. 1. Wetting front dispersion as a function of the dielectric constant (K′) and soil depth used in the TDR trace simulation program. The large squares mark the approximate midpoints between the locations of the dielectric constants of the wet (K'_w) and dry (K'_d) soil. These midpoints correspond with the wetting front measured on the clear wall of the cylinder. The depth used in Eq. (4) to calculate the upper boundary of the wetting front, (D_u), is marked on the right.

ting front. The optimization program uses a genetic algorithm (GA) (programs available on request from the authors). Genetic algorithms emulate evolution and are commonly used as optimization tools in engineering problems. Advantages of GAs include: (i) initial estimates are not important; (ii) several optimum parameter sets can be found if they exist; and (iii) the number of parameters to optimize can be very large (up to hundreds). A GA was chosen for this study because of the relatively large number of parameters to be fitted. This method is more robust for optimization of a large number of parameters than a gradient-based method (Yun et al., 2000). As the number of parameters increases, the response surface becomes less smooth and contains numerous local maxima and minima. Gradient-based methods such as the Newton-Raphson and Marquardt methods look for extremums, where the partial derivatives vanish and often get stuck in local minima (Yun et al., 2000).

The parameters to be optimized are represented as a binary array in the GA. The binary representations of all the parameters are concatenated into one string. This binary string represents the *chromosome* for one individual. Each chromosome consists of genes (e.g., bits), each gene being an instance of a particular allele (e.g., 0 or 1). For example, if the values of the parameters to be used for a particular iteration are 1, 2, and 3, then the chromosome is 000100100011. The optimization employs a population of single chromosomal individuals, each with a different binary representation of the parameters. The optimization criterion calculates the fitness of the chromosomes, and the individuals compete for the best fitness.

Individuals with better chromosomes have more chances to reproduce. In order to carry out "reproduction", genetic algorithms employ methods for moving from one population of chromosomes (e.g., strings of ones and zeroes, or bits) to a new population by using a kind of "natural selection" together with genetics-inspired operators of crossover and mutation. The selection operator chooses those chromosomes that will be allowed to reproduce. Crossover exchanges subparts of two chromosomes, roughly mimicking biological recombination between two single-chromosome organisms. Mutation randomly changes the allele values in some genes. Each iteration of selection, crossover, and mutation is called a generation. Usually, hundreds of generations are needed to produce a chromosome with a good fitness. More information on genetic algorithms can be found in Goldberg (1989).

In this study, the fitness (F_i) of an individual, i, is the inverse of the sum of squared deviations between measured and simulated wave traces summed over all the wave traces in an infiltration period:

$$F_i = \frac{1}{\sum_{i=1}^{n} \left(\sum_{j=1}^{251} (V_m - V_p)^2 \right)} \qquad (6)$$

Here n is the number of wave traces, V_m is the measured voltage, and V_p is the predicted voltage. The Tektronix 1502B cable tester samples 251 values of voltage for each wave trace. The fitness function is defined so that the highest fitness is assigned to the smallest squared error.

We used a FORTRAN version of a genetic algorithm called GAFORTRAN[3] This implementation uses tournament selection, in which all chromosomes have equal chances for reproduction, but the fitter of any two has a larger probability to become a parent. Elitism is allowed, which means that the algorithm is forced to allow the best individuals to become parents in each generation. The crossover is uniform and

[3]David L. Carroll, http://cuaerospace.com/carroll/ga.html

the allele exchange occurs in each bit position. To preserve the diversity in the population, individuals that are similar to many other individuals are punished, and individuals that are different are rewarded. As for any heuristic algorithm, internal parameters of the GA have to be found by trial and error, mostly to make computation time more bearable. We found that an increase in population size above 10 and number of generations greater than 300 did not change the solution. Default parameters of the GAFORTRAN were used for the probability of mutation (0.1) and crossover (0.5) and number of offspring per generation (2). It would not be likely that the parameters would differ greatly for other similar applications.

The parameters, K'_w, c, s, β, a and impedances of the handles and rods are coded in the initial population of individual chromosomes. The initial chromosomes are generated randomly, given the maximum and minimum values of the parameters (given as input) as well as the number of possible values between the maximum and minimum. A descritization parameter determines the potential precision of the distribution of parameter values. For example, if the parameter ranges from 1 to 100 and the number of possible values is 256, then the smallest difference between any two values is (100–1)/256 or 0.387. Thus, the number of possible values of a parameter to be fit will control the resolution of the final, fitted value. Other parameters to run the simulations, such as the dielectric constant of soil below the wetting front, the attenuation coefficients of the cable and handle, and the dielectric constant of the handle, are determined from measurements in the dry soil before infiltration and are held constant during fitting. The attenuation coefficients used for the cable and handle were $6.0e10^{-6}$ and $3.0e10^{-5}$, respectively, and the K′ of the handle was 2.6.

After the initial population of individual chromosomes is generated, the simulation of wave traces begins by decoding the parameters from the chromosome of the first individual back to the floating point number. The wetting depth for each measurement time is calculated according Eq. (4), with the time from the beginning of infiltration represented by the current wave trace. The distribution of the dielectric coefficient along the waveguides is calculated next using the current values of the parameters and Eq. (3). A wave trace is then simulated, and the program calculates the sum of squared deviations between the measured and simulated wave traces. This process continues through successive wave traces until the end of the infiltration period. The sums of squares are totaled for all of the wave traces, and a fitness function is calculated according to Eq. (6) for the current individual. This process is repeated for all the individuals in the population. Those with the highest fitness (F) are chosen for reproduction. A new population of individuals is generated, and the process is continued until the improvement in fitness is small. The wetting depth, D_w, is not optimized directly but is calculated from the optimized parameters, s, c, and β.

RESULTS AND DISCUSSION

Measured and predicted wave traces for three times are shown in Fig. 2. The simulated wave trace captures the features of the measured wave trace, especially the boundary between the wet and dry soil shown by arrows. The fitted parameters are given in Table 2. The impedances (Z) for the handle and waveguides do not differ greatly for the two infiltration runs. This is also true for the value of the parameter a that defines the attenuation in the waveguides in Eq. (2). The value for dispersivity is lower in the second infiltration than in the first. This reflects the differences in bulk density between the two samples. The parameters that describe the wetting front advance are also given in Table 2. The values of the coefficient and exponent are both lower for the second infiltration, reflecting the slower rate of infiltration.

The fitted values for K′ for the initially wet soils for the two infiltrations are 39.4 and 34.9. The values calculated from the manual calibration from Timlin and Pachepsky (1996) ($0.117\sqrt{K'} - 0.102$) for the loamy sand soil are 39.3 and 31.2 for the saturated water contents (based on total porosities in Table 1). The optimization method, therefore gives reasonable approximations of the dielectric constant. It is important to note that the water contents in this study are higher than those used in the calibration given in Timlin and Pachepsky (1996). Deviations from the relationship between water content and the square root of the apparent dielectric constant in the wet range are more common in soils with high clay content (Topp et al., 1980). In order to determine the wetting front water content profile and cumulative infiltration accurately, however, a separate calibration at the wet range would be needed to obtain correct water contents for the soil above the wetting front. The initial water content in the wetting zone during infiltration could be less than the saturation value

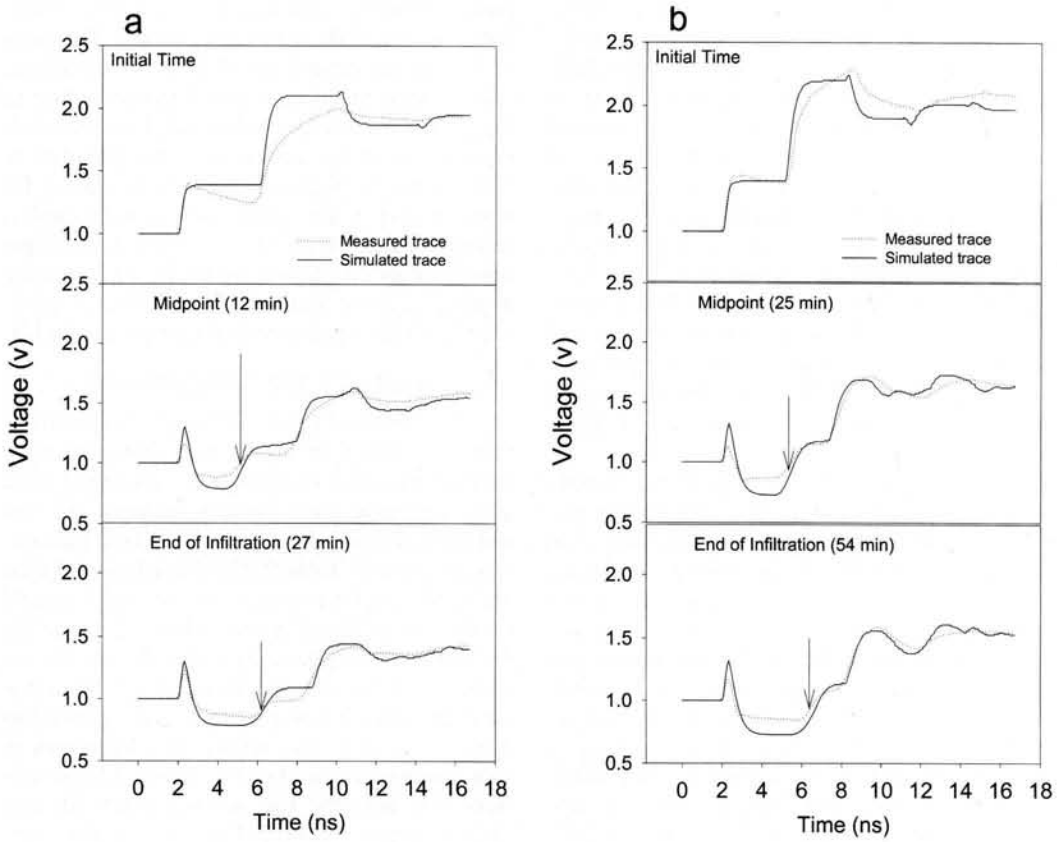

Fig. 2. Measured and simulated wave traces for the first (a) and second (b) infiltration experiments. Three times are shown: the beginning, half time, and the end of infiltration. The arrows point to the approximate location of the wetting front.

TABLE 2

Fitted parameters output by the optimization, including the impedances of the handle and waveguides, the attenuation coefficient for the waveguides in soil (α), the dielectric constant of the wet soil ahead of the wetting front (K_w), the dispersion coefficient for the wetting front (β), and the parameters that describe the rate of advance of the wetting front with time (s,c)

Infiltration no.	Impedance		Attenuation coefficient (α)	Dielectric constant of the wet zone	Dispersivity coefficient (β)	Parameters to describe wetting front advance (Eq. (4))		RMSE
	Handle	Rods		(K'_w)		s	c	
	Ω		cm^{-1}		$cm^2\ min^{-1}$	cm min^{-1}		volts
1	249.6	204.7	0.087	39.4	0.077	1.91	0.41	0.00462
2	274.2	170.5	0.048	34.9	0.047	1.77	0.38	0.00546

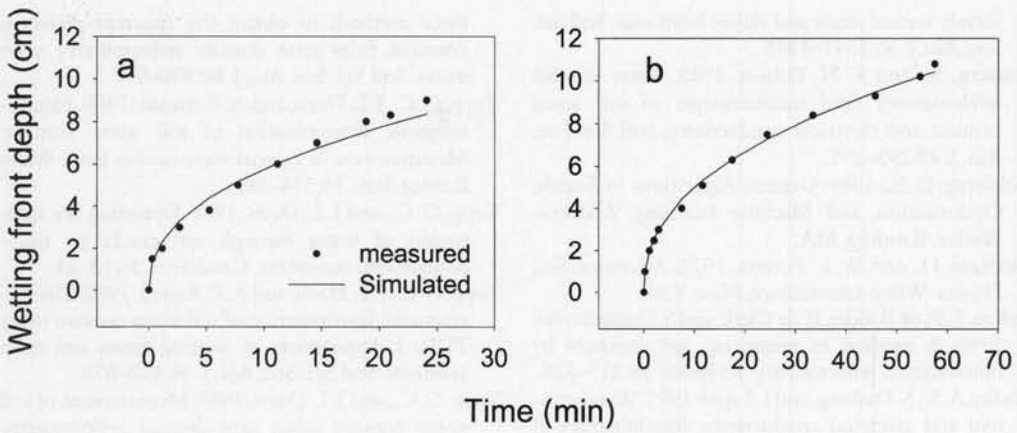

Fig. 3. Measured and calculated wetting front depth for the first (a) and second (b) infiltration experiments.

obtained from bulk density because of the effects of air entrapment (Constantz et al., 1988).

Measured and predicted wetting front depths as functions of time are shown in Fig. 3. The calculated wetting front depth is close to the measured depth for both tests. The first infiltration shows larger differences that may have been related to the low bulk density (Table 1) and attendant settling of soil during infiltration. The power functions fit both sets of infiltration data well. The root mean square errors for the prediction of wetting depths were 0.38 cm for the first trial and 0.20 cm for the second. Given the precision of the measured wetting front depth of 0.5 cm, this accuracy shows the precision of the method for capturing progression of the infiltrating front.

SUMMARY AND CONCLUSIONS

This paper describes the development and use of a TDR trace simulation model to calculate the depth of the wetting front during ponded infiltration. No knowledge of the relationship between water content and dielectric constant was needed. TDR wave traces were recorded during ponded infiltration into cylinders packed with a sandy loam soil. The waveguides were inserted vertically into the soil. Variation of the dielectric constant at the wetting front zone was accounted for by the model. The depth of the wetting front was calculated from the approximate midpoint between the locations of the fully wetted soil and dry soil. An optimization program that uses a genetic algorithm coupled to a TDR trace simulation model was used to fit a distribution of dielectric coefficients along the waveguides. The fitted parameters were the impedances of the handle and waveguides, an attenuation factor, dispersion parameter, dielectric constant of the wet soil, and parameters to describe the wetting front depth with time.

The calculated and measured wetting depths were similar for both infiltration tests. The model and optimization procedure works well and is promising as a method to automate measurements of ponded infiltration into soil. This setup is suited for a multiplexed arrangement to estimate wetting front depth under ponded infiltration at a large number of sites simultaneously. However, the method needs to be evaluated further in field soils. Both variations in soil properties and in water contents with depth before infiltration may impact the ability to detect a wetting front boundary from TDR wave traces. Further developments may include the possibility of tying the model with the Richards equation to calculate infiltration under time-varying boundary conditions.

REFERENCES

Ahuja, L. R., S. A. El-Swaify, and R. Rahman. 1976. Measuring hydrologic properties of soil with a double ring infiltrometer and multiple-depth tensiometers. Soil Sci. Soc. Am. J. 40:494–499.

Ali, A.-S. I., and D. Swartzendruber. 1994. An infiltration equation to assess cropping effects on soil water infiltration. Soil Sci. Soc. Am. J. 58:1218–1223.

Constantz, J. W., N. Herkelrath, and F. Murphy. 1988. Air encapsulation during infiltration. Soil Sci. Soc. of Am. J. 52:10–16.

Dasberg, S., and J. W. Hopmans. 1992. Time domain reflectometry calibration for uniform and nonuni-

formly wetted sandy and clayey loam soils. Soil Sci. Soc. Am. J. 56:1341–1345.

Dasberg, S., and F. N. Dalton. 1985. Time domain refelctometry field measurements of soil water content and electrical conductivity. Soil Sci. Soc. Am. J. 49:293–297.

Goldberg, D. E., 1989. Genetic Algorithms in Search, Optimization, and Machine Learning. Addison-Wesley, Reading, MA.

Kirkham, D., and W. L. Powers. 1972. Advanced Soil Physics. Wiley-Interscience, New York.

Ledieu, J., P. de Ridder, P. de Clerk, and S. Dautrebande. 1986: A method of measuring soil moisture by time-domain reflectometry. J. Hydrol. 88:319–328.

Nadler, A. S., S. Dasberg, and I. Lapid. 1991. Water content and electrical conductivity determination of layered soil profiles using TDR. Soil Sci. Soc. Am. J. 55:938–943.

Parkin, G. W., R. G. Kachanoski, D. E. Elrick, and R. G. Gibson. 1995. Unsaturated hydraulic conductivity measured by time domain reflectometry under a rainfall simulator. Water Resour. Res. 31:447–454.

Si, B., R. G. Kachanoski, F. Zhang, G. W. Parkin, and D. E. Elrick. 1999. Measurement of hydraulic properties during constant flux infiltration: Field average. Soil Sci. Soc. Am. J. 63:793–799.

Timlin, D. J., and Ya. Pachepsky. 1996. Comparison of three methods to obtain the apparent dielectric constant from time domain reflectometry wave traces. Soil Sci. Soc. Am. J. 60:970–977.

Topp, G. C., J. L. Davis, and A. P. Annan. 1980. Electromagnetic determination of soil water content: Measurements in coaxial transmission lines. Water Resour. Res. 16:574–582.

Topp, G. C., and J. L. Davis. 1981. Detecting the infiltration of water through soil cracks by time-domain reflectometery. Geoderma 26:13–23.

Topp, G. C., J. L. Davis, and A. P. Annan. 1982. Electromagnetic determination of soil water content using TDR: I. Applications to wetting fronts and steep gradients. Soil Sci. Soc. Am. J. 46:672–678.

Topp, G. C., and J. L. Davis. 1985. Measurement of soil water content using time-domain reflectometry (TDR): A field evaluation. Soil Sci. Soc. Am. J. 49:19–24.

Yanuka, M., G. C. Topp, S. Zegelin, and W. D. Zebchuk. 1988. Multiple reflection and attenuation of time-domain reflectometry pulses: Theoretical considerations for applications to soil and water. Water Resour. Res. 7:939–944.

Yun, I, L. A. Carastro, R. Poddar, M. A. Brooke, G. S. May, K. S. Hyun, and K. E. Pyun. 2000. Extraction of passive device model parameters using genetic algorithms. Etri J. 22:38–46.